

## Video Article

# Fabrication of Ultra-thin Color Films with Highly Absorbing Media Using Oblique Angle Deposition

Young Jin Yoo<sup>1</sup>, Gil Ju Lee<sup>1</sup>, Kyung-In Jang<sup>2</sup>, Young Min Song<sup>1</sup><sup>1</sup>School of Electrical Engineering and Computer Science, Gwangju Institute of Science and Technology<sup>2</sup>Department of Robotics Engineering, Daegu Gyeongbuk Institute of Science and TechnologyCorrespondence to: Kyung-In Jang at [kijang@ggist.ac.kr](mailto:kijang@ggist.ac.kr), Young Min Song at [ymsong@ggist.ac.kr](mailto:ymsong@ggist.ac.kr)URL: <https://www.jove.com/video/56383>DOI: [doi:10.3791/56383](https://doi.org/10.3791/56383)

Keywords: Engineering, Issue 126, optoelectronics (applications), Electronics and Electrical Engineering, coloration, ultra-thin, thin-film, highly absorbent media, optical coating, oblique angle deposition

Date Published: 8/29/2017

Citation: Yoo, Y.J., Lee, G.J., Jang, K.I., Song, Y.M. Fabrication of Ultra-thin Color Films with Highly Absorbing Media Using Oblique Angle Deposition. *J. Vis. Exp.* (126), e56383, doi:10.3791/56383 (2017).

## Abstract

Ultra-thin film structures have been studied extensively for use as optical coatings, but performance and fabrication challenges remain. We present an advanced method for fabricating ultra-thin color films with improved characteristics. The proposed process addresses several fabrication issues, including large area processing. Specifically, the protocol describes a process for fabricating ultra-thin color films using an electron beam evaporator for oblique angle deposition of germanium (Ge) and gold (Au) on silicon (Si) substrates. Film porosity produced by the oblique angle deposition induces color changes in the ultra-thin film. The degree of color change depends on factors such as deposition angle and film thickness. Fabricated samples of the ultra-thin color films showed improved color tunability and color purity. In addition, the measured reflectance of the fabricated samples was converted into chromatic values and analyzed in terms of color. Our ultra-thin film fabricating method is expected to be used for various ultra-thin film applications such as flexible color electrodes, thin film solar cells, and optical filters. Also, the process developed here for analyzing the color of the fabricated samples is broadly useful for studying various color structures.

## Video Link

The video component of this article can be found at <https://www.jove.com/video/56383/>

## Introduction

In general, the performance of thin-film optical coatings is based on the type of optical interference they produce, such as high reflection or transmission. In dielectric thin-films, optical interference can be obtained simply by satisfying conditions such as quarter wave thickness ( $\lambda/4n$ ). Interference principles have long been used in various optical applications such as Fabry-Perot interferometers and distributed Bragg reflectors<sup>1,2</sup>. In recent years, thin film structures using highly absorbent materials such as metals and semiconductors have been widely studied<sup>3,4,5,6</sup>. Strong optical interference can be obtained by thin-film coating an absorbent semiconductor material on a metal film, which produces non-trivial phase changes in the reflected waves. This type of structure allows ultra-thin coatings which are considerably thinner than dielectric thin-film coatings.

Recently, we studied ways of improving the color tunability and color purity of highly absorbent thin-films using porosity<sup>7</sup>. By controlling the porosity of the deposited film, the effective refractive index of the thin-film medium can be changed<sup>8</sup>. This change in the effective refractive index allows the optical characteristics to be improved. Based on this effect, we designed ultra-thin color films with different thicknesses and porosities by calculations using rigorous coupled wave analysis (RCWA)<sup>9</sup>. Our design presents colors with different film thicknesses at each porosity<sup>7</sup>.

We employed a simple method, oblique angle deposition, to control the porosity of highly absorbent thin-film coatings. The oblique angle deposition technique basically combines a typical deposition system, such as an electron beam evaporator or thermal evaporator, with a tilted substrate<sup>10</sup>. The oblique angle of incident flux creates atomic shadowing, which produces areas that the vapor flux cannot reach directly<sup>11</sup>. The oblique angle deposition technique has been widely used in various thin-film coating applications<sup>12,13,14</sup>.

In this work, we detail the processes for fabricating ultra-thin color films by oblique deposition using an electron beam evaporator. Also, additional methods for large-area processing are presented separately. In addition to the process steps, some notes that should be taken into consideration during the fabrication process are explained in detail.

We also review processes for measuring the reflectance of the fabricated samples and converting them into color information for analysis, so that they can be expressed in CIE color coordinates and RGB values<sup>15</sup>. Furthermore, some issues to consider in the fabrication process of ultra-thin color films are discussed.

## Protocol

Caution: Some chemicals (*i.e.*, buffered oxide etchant, isopropyl alcohol, *etc.*) used in this protocol can be hazardous to health. Please consult all relevant material safety data sheets before any sample preparation takes place. Utilize appropriate personal protective equipment (*e.g.*, lab coats, safety glasses, gloves, *etc.*) and engineering controls (*e.g.*, wet station, fume hood, *etc.*) when handling etchants and solvents.

### 1. Preparation of the Si Substrate

1. Using a diamond cutter, cut a 4 inch silicon (Si) wafer into 2 cm x 2 cm sized squares. To make colored samples, the substrate is typically cut 2 cm x 2 cm, but can be larger, depending on the size of the sample holder used for oblique angle deposition.
2. To remove native oxide using Polytetrafluoroethylene (PTFE) dipper, dip the cleaved Si substrates in buffered oxide etchant (BOE) for 3 s.  
**Caution:** Please wear appropriate protection for safety.
3. **Clean the cleaved Si substrates sequentially in acetone, isopropyl alcohol (IPA), and deionized (DI) water for 3 s each.**
  1. Using PTFE cleaning jig, sonicate the cleaved Si substrates with acetone in an ultrasonic bath for 3 min at a frequency of 35 kHz.
  2. To remove the acetone, rinse the cleaved Si substrates with IPA.
  3. As the last step of cleaning, rinse the cleaved Si substrates with DI water.
4. To remove moisture, dry the clean substrate with a nitrogen blow gun while holding it with forceps.

### 2. Deposition of the Au Reflector

1. Using forceps and carbon tape, fix the cleaned Si substrates onto a flat sample holder and place the holder into the chamber of the electron beam evaporator with Ti and Au sources.
2. Evacuate the chamber for 1 h to reach high vacuum. The base pressure of the vacuum chamber should be  $4 \times 10^{-6}$  Torr.
3. Deposit the Ti layer as an adhesion layer to a thickness of 10 nm with 5 - 7% of electron beam power controlled in manual mode at a DC voltage of 7.5 kV, which gives a deposition rate of 1 Å/sec.  
Note: A Cr layer of the same thickness, instead of a Ti layer, can be deposited as the adhesion layer.
4. Deposit the Au layer as a reflection layer to a thickness of 100 nm with 13-15% of electron beam power controlled in manual mode at a DC voltage of 7.5 kV, which gives a deposition rate of 2 Å/sec.  
Note: The thickness of the Au reflection layer can be greater than 100 nm. A thickness of 100 nm is deposited here to make the reflection layer as thin as possible while maintaining the optical properties of the Au.
5. After the Au layer deposition, vent the chamber and take out the samples. They will need to be reloaded with the inclined sample holder for the oblique angle deposition.

### 3. Preparation of the Inclined Sample Holder for Oblique Angle Deposition

Note: There are several methods that can be used for oblique deposition, such as the z-axis rotating chuck<sup>16</sup>, but this requires equipment modification and films can only be deposited at one angle at a time. To efficiently observe the changes in color produced by different deposition angles, we used sample holders that inclined the samples at different angles. For precision, the inclined sample holder can be made using metal processing equipment. However, in this paper, we introduce a simple method that can be easily followed.

1. Prepare a metal plate made of an easily bendable metal such as aluminum.
2. Cut the metal plate into three 2 cm x 5 cm pieces.
3. Fix the metal piece to the floor alongside a protractor, hold the short side and bend the metal to the desired deposition angle (*i.e.*, 30°, 45°, and 70°).
4. Attach the bent metal pieces to the 4 inch sample holder using carbon tape.

### 4. Oblique Angle Deposition of Ge Layer

Note: In this section, refer to the schematic diagrams in **Figure 1** of the samples deposited on the inclined sample holders, and porous Ge films, following oblique angle deposition.

1. Fix the four Au deposited samples with carbon tape to an inclined sample holder at angles of 0°, 30°, 45°, and 70°, respectively.
2. Load the Au-deposited samples on the inclined sample holder into the electron beam evaporator with a Ge source for oblique angle deposition.
3. Evacuate the chamber for 1 h to reach high vacuum. The base pressure of the vacuum chamber should be  $4 \times 10^{-6}$  Torr.
4. Deposit the Ge layer as a coloring layer with 6 - 8% of electron beam power controlled in manual mode at a DC voltage of 7.5 kV, which gives a deposition rate of 1 Å/sec. The deposition thicknesses of the Ge layer on the four samples are 10 nm, 15 nm, 20 nm, and 25 nm, respectively.  
Note: The deposition thicknesses of 10 nm, 15 nm, 20 nm, and 25 nm were selected to facilitate comparison of the color changes for each deposition angle. A different angle and thickness (5 - 60 nm) can be chosen to achieve a particular color.
5. After the Ge layer deposition, vent the chamber and take out the samples.

## 5. Oblique Angle Deposition Process for Large Areas

Note: If the size of the sample used for oblique angle deposition is small, it can be fabricated by the process detailed in step 4. However, if the size of the sample to be fabricated is large, it becomes difficult to maintain film uniformity due to variation in the evaporation flux along the z-axis<sup>16</sup>. Therefore, a separate additional process, step 5, is required to fabricate larger samples and achieve a uniform color.

- For a 2 inch wafer, after depositing the Au layer on the large sample in step 2, fix the Au-deposited large sample to the 45° inclined sample holder.  
Note: Since our inclined sample holder is designed to fit small samples, loading large samples at all the angles (*i.e.*, 0°, 30°, 45°, and 70°) will create interference between samples. Therefore, to obliquely deposit large-sized samples at various angles in one process, it is necessary to have an inclined sample holder suitable for large-sized samples.
- Load the Au-deposited large sample on the inclined sample holder into the electron beam evaporator with a Ge source for oblique angle deposition.  
Note: When loading the sample, the second deposition layer must be deposited in the same direction as the first deposition, so note the direction of the loaded sample. For convenience, it is recommended that the sample holder is loaded facing the front of the chamber.
- Evacuate the chamber for 1 h to reach high vacuum. The base pressure of the vacuum chamber should be  $4 \times 10^{-6}$  Torr.
- Deposit the Ge layer as a coloring layer to a deposition thickness of 10 nm, which is half of the target thickness of 20 nm, with 6 - 8% of electron beam power controlled in manual mode at a DC voltage of 7.5 kV, which gives a deposition rate of 1 Å/sec.
- After the deposition of the first Ge layer is finished, vent the chamber and take out the sample, because the sample needs to be repositioned and reloaded.
- Fix the sample to the inclined sample holder in a position which is upside down with respect to the position of the first deposition.
- Load the sample on the inclined sample holder with the Ge source so that the holder faces in the same direction as the first deposition.
- Evacuate the chamber for 1 h to reach high vacuum. The base pressure of the vacuum chamber should be  $4 \times 10^{-6}$  Torr.
- Deposit the Ge layer as a coloring layer to a deposition thickness of 10 nm, which is half of the target thickness of 20 nm, with 6 - 8% of electron beam power controlled in manual mode at a DC voltage of 7.5 kV, which gives a deposition rate of 1 Å/sec.
- After the Ge layer deposition, vent the chamber and take out the sample.

### Representative Results

**Figure 2a** shows images of the 2 cm x 2 cm fabricated samples. The samples were fabricated so that the films had different thicknesses (*i.e.*, 10 nm, 15 nm, 20 nm, and 25 nm) and were deposited at different angles (*i.e.*, 0°, 30°, 45°, and 70°). The color of the deposited films changes depending on the combination of both the thickness of the samples and the deposition angle. The changes in color result from changes in the porosity of the film. Depending on the deposition angle, inclined arrays of individual nano-columns are created on the substrate, as shown in the left SEM images of **Figure 2**. From the experimental results, it can be seen that at higher deposition angles, the color change for each deposition angle is less pronounced.

**Figure 2b** shows the results of reflectance measurements of the fabricated samples. The color is changed by a shift in the minimum dip of reflectance. As shown by the color change in **Figure 2a**, the reflection dip has shifted slowly at higher deposition angles. With each Ge layer thickness, the reflection dip changes with the deposition angle. The color is changed by these shifts in the reflection dip.

To analyze the fabricated samples from a color perspective, the measured reflectances need to be converted to chromatic values. For conversion to chromatic values, in our calculations, the CIE 1931 standard observer function, the most commonly used color matching function, was employed<sup>13</sup>. In the calculation, the measured reflectance is multiplied by the color matching function as a spectral power distribution. **Figure 3a** demonstrates the spectral response with the color matching function of the measured reflectance of samples with different deposition angles (*i.e.*, 0°, 30°, 45°, and 70°) and a Ge layer thickness of 15 nm. By integrating these spectral responses, the tristimulus values of X, Y, and Z, which are the basic parameters for expressing color information, can be obtained. In the CIE color coordinates, the chromaticity of a color is specified by the two derived parameters *x* and *y*, and the normalized values of all three tristimulus values using the following equations:

$$x = \frac{X}{X + Y + Z}$$

$$y = \frac{Y}{X + Y + Z}$$

Based on these equations, **Figure 3b** shows the chromaticity of samples with different deposition angles in the CIE coordinate system.

**Figure 4a** shows the chromatic values after they have been converted from the measured reflectance in **Figure 3a** into the CIE color coordinate system. For comparison, the calculated results were also plotted, as shown by the dashed lines. In the calculation, the effective indices of Ge were calculated based on the porosities expected for each deposition angle<sup>7</sup>. Then, using these effective indices, the reflectance values were calculated by rigorous coupled wave analysis (RCWA)<sup>9</sup>. Compared using the CIE coordinate system, the experimental results were well matched to the calculated results.

Comparing the ranges of the chromatic values of the samples, those samples with high deposition angles exhibited a wider chromatic range. This means that the range of color expressions was wide, with higher color purity. The higher color purity at higher deposition angles is attributed to the reduction in surface reflection resulting from the higher porosity due to deposition at higher angles.

The color information converted from the reflectance can be converted into RGB values to represent colors<sup>15</sup>. **Figure 4b** shows the color representation after converting the color information from the measured reflectance of the samples to RGB values. The photographs may not

accurately represent the true sample colors, due to differences in illumination or other conditions, but the overall tendency in color change from sample to sample can be seen.

**Figure 5** shows images of the samples fabricated on a 2 inch wafer, using the large area process. When fabricating a large sample, the deposited thickness differs depending on the position of the surface. A solution to this problem is to perform the deposition in two steps, as detailed in step 5 of the protocol. The first layer, with half of the desired thickness, is deposited at a positive deposition angle, and the second half is deposited at a negative deposition angle. In this way, by depositing at positive and negative angles, the differences in thickness will compensate each other, and a uniform thickness can be obtained.

Our targets were 20 nm and 40 nm thickness at a deposition angle of 45°, however, the results showed thicker deposits. This is because the compensated average thickness was formed in the vertical direction at a position closer to the source than the sample holder<sup>16</sup>. Thus, when fabricating on a large scale using this method, it should be expected that the deposited film will be thicker than the target thickness.

**Figure 6** depicts images of the fabricated samples at different viewing angles, and measured reflectance at different incident angles. As shown in the images, there is little change in color based on viewing angles. The minimum dips of the measured reflectance values at different angles were also hardly shifted by the incident angles. Basically, as these coatings are much thinner than the wavelengths of the incident light, there is little phase difference resulting from the increased angle of incidence compared with the case of normal incidence.

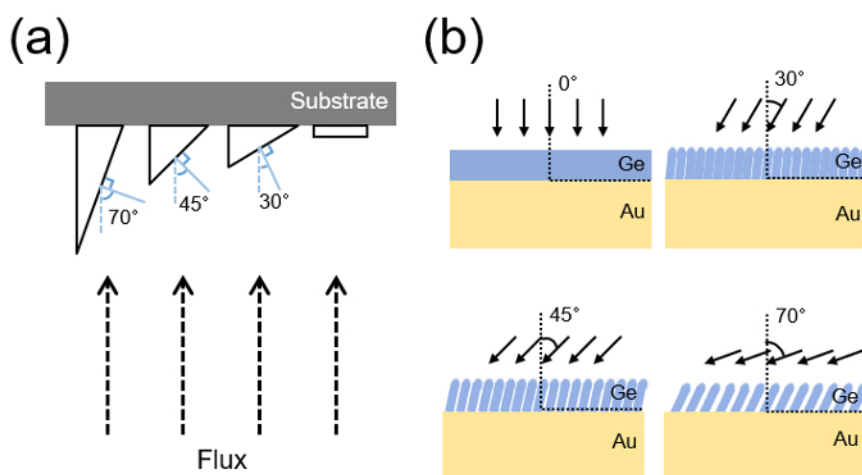


**Figure 1:** Schematic diagrams of (a) the samples deposited on the inclined sample holders, and (b) porous Ge films created by the oblique angle deposition. [Please click here to view a larger version of this figure.](#)

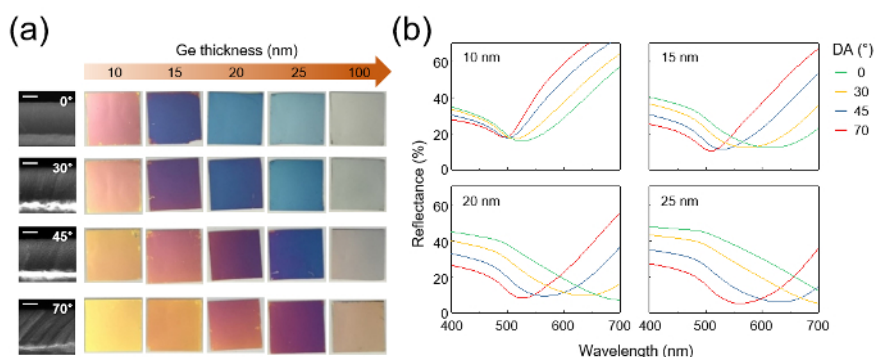


**Figure 2:** (a) Images of the samples fabricated at different deposition angles (*i.e.*, 0°, 30°, 45°, and 70°) with different Ge thickness (*i.e.*, 10 nm, 15 nm, 20 nm, 25 nm, and 100 nm). Left, gray-scale figures show scanning microscopy images corresponding to the samples with Ge thickness of 200 nm for better showing the morphology. Scale bar = 100 nm. (b) Measured reflectance spectra for each Ge thickness (*i.e.*, 10 nm, 15 nm, 20 nm, and 25 nm) with different deposition angles (*i.e.*, 0°, 30°, 45°, and 70°). [Please click here to view a larger version of this figure.](#)

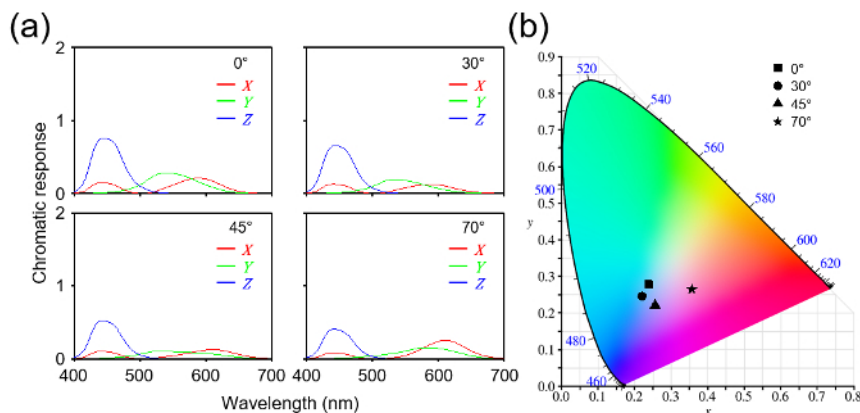


**Figure 3:** (a) Chromatic response of the tristimulus values and (b) the CIE plot with different deposition angles (*i.e.*, 0°, 30°, 45°, and 70°) at a Ge thickness of 20 nm. [Please click here to view a larger version of this figure.](#)

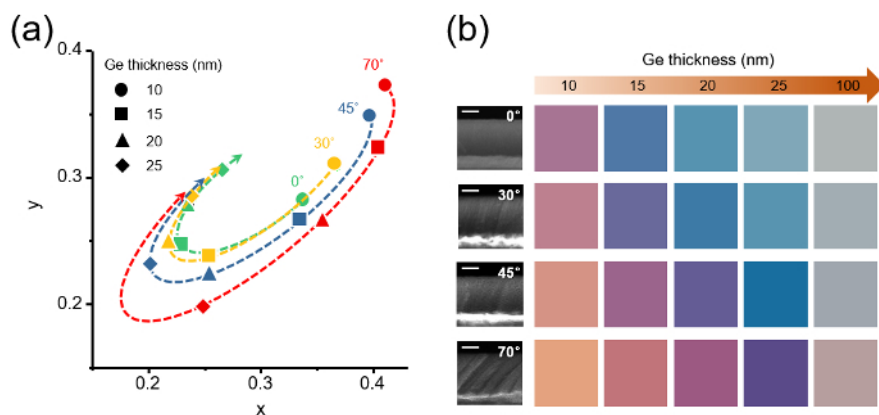


**Figure 4:** (a) Chromatic values in the CIE coordinates from the measured reflectance values of the fabricated samples, showing the calculated results. (b) Color representation based on the measured reflectances of the fabricated samples. Left, gray-scale figures show scanning microscopy images corresponding to the samples with Ge thickness of 200 nm for better showing the morphology. Scale bar = 100 nm. This figure has been reproduced from 7 with permission from the Royal Society of Chemistry. [Please click here to view a larger version of this figure.](#)

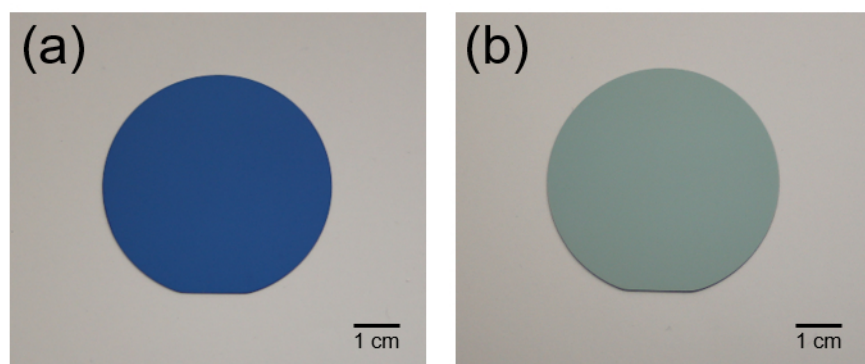


**Figure 5:** Images of Fabricated Samples on 2-inch Wafer with Different Ge Thicknesses of (a) 20 nm, and (b) 40 nm at a Deposition Angle of 45°.

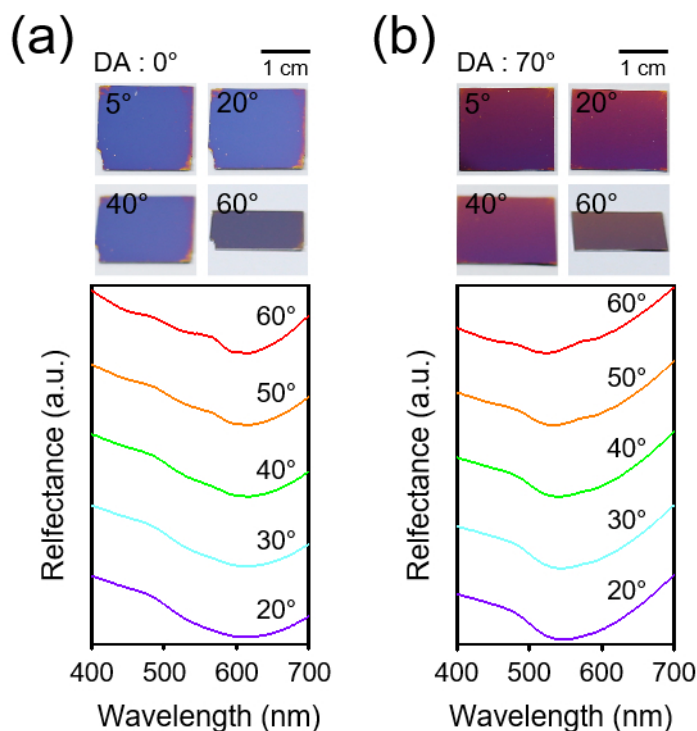


**Figure 6:** Images with Different Angles of View from 5° to 60° and Measured Reflectance Spectra at Oblique Angles from 20° to 60° of Fabricated Samples with (a) a Ge Thickness of a 15 nm at a Deposition Angle of 0°, (b) a Ge Thickness of a 25 nm at a Deposition Angle of 70°. This figure has been reproduced from Y. J. Yoo *et al.*<sup>7</sup>, with permission from the Royal Society of Chemistry.

## Discussion

In conventional thin film coatings for coloration<sup>3,4,5,6</sup>, the color can be controlled by altering different materials and adjusting the thickness. The choice of materials with different refractive indices is limited for tuning various colors. To relax this limitation, we exploited the oblique angle deposition to thin-film color coating. Depending on the deposition angle, the porosity of the Ge layer is changed by atomic shadowing<sup>11</sup>, as shown in **Figure 1b**. The porosity applied to the Ge thin-film causes a change in the effective index of the Ge layer<sup>7</sup>. The phase change of the propagating light in the Ge medium varies with the change of the effective index by the oblique angle deposition. As a result, the color changes with different interference conditions in the visible wavelengths. Especially in our ultra-thin color films, the low effective index at a highly oblique deposition angle enhanced the color purity with lower surface reflection and the tunability with a smaller phase change.

In our protocol, step 4 is the most critical process for coloration. To successfully execute step 4, consider that the film quality is a critical factor in thin film optical coating coloration. The film quality can change the refractive index, and subtly affects the coloration. The film quality depends on the nature and conditions of the deposition equipment. In our case, an electron beam evaporator was used as the deposition equipment, and constant pressure and deposition rates were maintained to ensure film stability. Furthermore, we measured the optical constants of the thin films deposited under these constant conditions, and by using the measured optical constants, the color of the thin film could be predicted and analyzed. To achieve an exact desired color and to tune the color using film thickness, ensure the stability of conditions, such as the pressure and deposition rate of the deposition equipment. Especially, in the case of different equipment, the various conditions of the equipment need to be optimized for tuning ultra-thin color films.

In the large area oblique angle deposition process, film deposition is non-uniform because of the vertical difference between the source and the substrate. In the electron beam evaporation process, the vapor flux density varies in the vertical direction from the source. At high oblique angles, there is a vertical difference depending on the position of the substrate, which causes flux density to be differently deposited depending on the surface position.

The process detailed in step 5 of the protocol was developed to compensate for this. This method is simple and can be easily followed without modifying the equipment. However, as mentioned in the results section, the process tends to result in greater film thickness than the target thickness. Another large-area process method that can solve this thickness problem is to modify the chuck in the chamber where the sample is loaded so that it rotates in the z-axis. When the sample is loaded at the center of the z-axis rotation, the center of the sample will always remain a constant distance from the source. Therefore, even with the deposition at positive and negative angles, a uniform thickness can be achieved. Furthermore, it should be noted that the oblique angle of the sample can be changed while maintaining the vacuum because the chuck is rotatable in the z-axis inside the chamber.

In conclusion, we have presented a process for fabricating ultra-thin color films using oblique angle deposition with an electron beam evaporator. In addition, we detailed a method for converting the measured optical properties of the fabricated samples into color information and analyzed them in terms of color with their CIE coordinates. This process used to measure and analyze the colors of the fabricated samples can also be

useful for the analysis of various other coloring structures. In this study, changes in color were observed depending on the thickness of the ultra-thin film and the deposition angle. Our ultra-thin color structures can be widely used for various thin-film applications such as flexible color electrodes, thin film solar cells, and optical filters.

## Disclosures

The authors have nothing to disclose.

## Acknowledgements

This research was supported by Unmanned Vehicles Advanced Core Technology Research and Development Program through the Unmanned Vehicle Advanced Research Center (UVARC) funded by the Ministry of Science, ICT and Future Planning, the Republic of Korea (2016M1B3A1A01937575)

## References

1. Macleod, H.A. *Thin-film optical filters*. Institute of Physics Publishing, 3rd ed. (2001).
2. Baumeister, P.W. *Optical Coating Technology*. SPIE Press, Bellingham, Washington. (2004).
3. Kats, M.A., Blanchard, R., Genevet, P., and Capasso, F. Nanometre optical coatings based on strong interference effects in highly absorbing media, *Nat. Mater.* **12**, 20–24 (2013).
4. Kats, M.A. et al., Ultra-thin perfect absorber employing a tunable phase change material, *Appl. Phys. Lett.* **101** (22), 221101 (2012).
5. Lee, K.T., Seo, S., Lee, J.Y., and Guo, L.J. Strong resonance effect in a lossy medium-based Optical Cavity for angle robust spectrum filters, *Adv. Mater.* **26** (36), 6324–6328 (2014).
6. Song, H., et al., Nanocavity enhancement for ultra-thin film optical absorber, *Adv. Mater.* **26** (17), 2737–2743 (2014).
7. Yoo, Y. J., Lim, J. H. Lee, G. J., Jang, K.I., and Song, Y.M. Ultra-thin films with highly absorbent porous media fine-tunable for coloration and enhanced color purity, *Nanoscale*. **9** (9), 2986–2991 (2017).
8. Garahan, A., Pilon, L., Yin, J., and Saxena, I. Effective optical properties of absorbing nanoporous and nanocomposite thin films, *J. Appl. Phys.* **101** (1), 014320 (2007).
9. Moharam, M.G. Coupled-wave analysis of two-dimensional dielectric gratings, *Proc. SPIE*. **883**, 8–11 (1988).
10. Robbie, K., Sit, J.C., and Brett, M.J. Advanced techniques for glancing angle deposition, *J. Vac. Sci. Technol. B*. **16** (3), 1115–1122 (1998).
11. Hawkeye, M.M., and Brett, M.J. Glancing angle deposition: Fabrication, properties, and applications of micro- and nanostructured thin films, *J. Vac. Sci. Technol. A*. **25** (5), 1317–1335 (2007).
12. Jang, S.J., Song, Y.M., Yu, J.S., Yeo, C.I., and Lee, Y.T. Antireflective properties of porous Si nanocolumnar structures with graded refractive index layers, *Opt. Lett.* **36** (2), 253–255 (2011).
13. Jang, S.J., Song, Y.M., Yeo, C.I., Park, C.Y., and Lee, Y.T. Highly tolerant a-Si distributed Bragg reflector fabricated by oblique angle deposition, *Opt. Mater. Exp.* **1** (3), 451–457 (2011).
14. Harris, K.D., Popta, A.C.V., Sit, J.C., Broer, D.J., and Brett, M.J. A Birefringent and Transparent Electrical Conductor, *Adv. Funct. Mater.* **18** (15), 2147–2153 (2008).
15. Fairman, H.S., Brill, M.H., and Hemmendinger, H. How the CIE 1931 color-matching functions were derived from Wright-Guild data, *Color Research & Application*. **22** (1), 11–23 (1997).
16. Oliver, J.B., et al., Electron-beam-deposited distributed polarization rotator for high-power laser applications, *Opt. Exp.* **22** (20), 23883–23896 (2014).